Design and Performance Analysis of Preamble Sequences for 5G RACH and Effect of Obstacles and Mobility on RACH Performance in 5G NR

PROJECT REPORT

Submitted by

SAGAR PAWAR

in partial fulfillment of the requirements

for the award of the degree of

MASTER OF TECHNOLOGY

Department Of Electrical Engineering

INDIAN INSTITUTE OF TECHNOLOGY MADRAS

JUNE 2021

DEPARTMENT OF ELECTRICAL ENGINEERING

INDIAN INSTITUTE OF TECHNOLOGY MADRAS

2021

CERTIFICATE

This is to certify that this thesis (or project report) entitled ***"Design and Performance Analysis of Preamble Sequences for 5G RACH and Effect of Obstacles and Mobility on RACH Performance in 5G NR"*** submitted by **SAGAR PAWAR** to the Indian Institute of Technology Madras, for the award of the degree of **Masters of Technology** is a bona fide record of the research work done by him under my supervision. The contents of this thesis (or project report), in full or in parts, have not been submitted to any other Institute or University for the award of any degree or diploma..

Dr. T. G. Venkatesh
Research Guide
Associate Professor
Department of Electrical Engineering
IIT Madras 600036

Acknowledgment

First and foremost, I would like to express my deepest gratitude to my guide, **Dr. T. G. Venkatesh**, Associate Professor, Department of Electrical Engineering, IIT Madras, for providing me an opportunity to work under him. I would like to express my deepest appreciation for his patience, valuable feedbacks, suggestions and motivations.

I convey my sincere gratitude to **Lokesh Bommisetty**, PhD Scholar, IIT Madras, for all his suggestions and support during the entire course of the project. Throughout the course of the project he offered immense help and provided valuable suggestions which helped me in completing this project.

I would like to extend my appreciation to all my friends for their help and support in completing my project successfully.

Abstract

5G NR employs a Random Access (RA) Procedure for up-link synchronization between User Equipment (UE) and Base Station (gNB) that requires a preamble to be transmitted by UE. However, the widely used Zadoff-Chu sequence (ZC-seq) for preamble generation has limitations in terms of the total number of preambles generated. The limited number of preambles causes the reuse of preambles, which increases the probability of collision. Hence, other sequences have been explored for preamble generation. In our work, we present the comparison between Zadoff-Chu, m-sequence and All-top sequence and their detection performance in RA procedure for a different number of receive antennas. We use the concept of cover sequences to get different combinations of Zadoff-Chu, m and All-top sequences for increased preamble capacity. We propose a new candidate sequence called $mAll$ with a higher preamble capacity than the proposed sequences in the literature. The properties of Random Access Preambles such as the periodic correlation, false-alarm probability and detection probability are analyzed for different preamble sequences. We explore the Peak to Average Power Ratio (PAPR) and Cubic Metric(CM) for these sequences, as these are essential parameters to be considered during transmission. 3GPP has specified the use of millimeter waves (mmWave) for communication in 5G NR, which are highly directional. The high directionality of such waves necessitates the use of beamformed signals, which can be directed towards a particular direction. The User Equipment (UE) needs to form a beam pair with gNB to start the RACH procedure for up-link connection establishment. Initiating the RACH procedure requires a preamble to be transmitted by the UE. We analyze the effects of user mobility, Line of Sight and Non-Line of sight conditions, effects of obstacles on the Beam Failure Probability and RACH success probability.

Contents

List of Figures

List of Tables

ABBREVIATIONS

RA	Random Access
UE	User Equipment
gNB	Base Station
ZC	Zadoff-Chu
PAPR	Peak to Average Power Ratio
CM	Cubic Metric
eMBB	Enhanced Mobile Broadband
URLLC	Ultra Reliable Low Latency Communications
mMTC	Massive Machine Type Communication
RACH	Random Access Channel
FR1/2	Frequency Range 1/2
PSS	Primary Synchronisation Signal
SSS	Secondary Synchronisation Signal
PCI	Physical Cell Identity
CSR	Cell Specific Reference Signal
mmWave	Millimeter Waves
3GPP	3^{rd} Generation Partnership Project
LOS	Line of Sight
NLOS	Non Line of Sight
SNR	Signal to Noise Ratio
PPP	Poisson Point Process
MAC	Media Access Control
CAZAC	Constant Amplitude Zero Auto Correlation
ZCZ	Zero Correlation Zone
LCZ	Low Correlation Zone

P(detection)	Probability of Detection
P(false)	Probability of False-Alarm
PrCapacity	Preamble Capacity
PA	Power Amplifier
PDP	Power Delay Profile
CSI-RS	Channel State Information- Reference Signal
RSRP	Reference Signal Received Power
SRS	Sounding Reference Signal
mZC	m-sequence combined with ZC sequence
aZC	All-Top sequence combined with ZC sequence
$mALL$	m-sequence combined with All-Top sequence
LFSR	Linear Feedback Shift Register
FFT	Fast Fourier Transform
IFFT	Inverse Fast Fourier Transform
$P(NLOS)$	Probability of non line of sight
$P(failure)$	Probability of beam failure
UMa	Urban Macro

Chapter 1

Introduction

1.1 Introduction to 5G

The deployment of 5G NR is a step forward for providing Enhanced Mobile Broadband (eMBB), Ultra Reliable Low Latency Communications (URLLC) and Massive Machine Type Communications(mMTC). Enhanced Mobile Broadband (eMBB) have requirements of data rates up to 10 to 20 Gbps with high mobility support of User Equipment (UE). Ultra Reliable Low Latency Communications (URLLC) require robust connectivity and very low end to end latency of 5 ms. Massive Machine Type Communications(mMTC) aims for density of One million connections per square kilometer for IOT devices with low power requirements [1].

3GPP, in its Release 15, has defined two frequency ranges for operations which are FR1 band (Sub-6 GHz) and FR2 (millimetre wave). The Sub-6 band is already in use in LTE, which gives us a larger coverage area with low directionality. The use of mmWave in 5G NR is a key point in achieving higher throughput and supporting higher mobility speeds for UE. Nevertheless, the use of mmWave comes with its

merits and demerits. mmWaves allow for higher sub-carrier spacing which in turn support higher bandwidths. mmWave being highly directional results in lower multi-paths which result in simpler and faster estimators. However, these advantages come with a cost of being suffered from higher path losses with distances and the need for Line of Sight communication for best-case scenarios.

For a UE to establish an uplink connection, Random Access (RA) procedure is initiated by UE after satisfying a few conditions. RA initiation requires the down-link connection to be established, where timing synchronisation between gNB and UE is essential. The downlink synchronisation is done with the help of Primary Synchronisation Signal (PSS) and Secondary Synchronisation Signals (SSS), using which the UE acquires information about Physical Cell Identity (PCI) and Cell Specific Reference Signal (CSR) and resource allocations. Using this information, UE initiates RA procedure to establish an uplink with the gNB.

One of the key components of 5G is mmWave for achieving higher throughput. This is achieved by carefully creating a beam which is highly directional. A directed link is formed between UE and gNB by forming beam pairs. The beam pair formation is essential for UE in order to initiate the RACH procedure for up-link establishment. The total frequency range defined in [2] is 0.5 GHz to 100 GHz. The mmWave band define by 3GPP is 24.25 - 52.6 GHz. Use of such high frequency wave allow us to have a larger bandwidth for transmission thus improving data rates. But the demerit of such high frequency signals is high propagation losses. Propagation loss is inversely proportional to the square of the frequency. Therefore as we increase frequency the propagation loss increases rapidly with distance. In case of mmWave, this limits the range of transmission, thus limiting the coverage area. mmWave are also prone to higher losses due to obstacles. Both these limitations of mmWave have the effect on beam pair formation.

The best case scenario for formation of beam pairs is Line of Sight (LOS) connection, where UE is in direct line of sight of the gNB. But this case is only possible for open areas like open stadiums, tracks, roads or rural areas where obstacles density is less. In an urban set setup, where there are buildings, obstacles all around the

UE often goes in Non Line of Sight (NLOS) condition. In NLOS state, beam pairs still can be formed via reflections and multi-paths. But as the UE moves through obstacles, the signal experiences propagation loss and fading. This degradation in signal quality may lead to beam failure if the quality measure is beyond some threshold. As the beam failure occurs, UE is needed to initiate a RACH procedure again. At each RACH instance, UE transmits a preamble toward gNB, and based on the detection at gNB, the RACH procedure can be declared as success and failure. If the gNB is not able to detect the said preamble transmitted by UE in time, the RACH will be declared as failure and UE will initiate the RACH procedure again.

1.2 Motivation

The main component for the initiation of RA procedure is a preamble. The preamble is a fixed length sequence that is primarily used for uplink synchronisation. In LTE, Zadoff-Chu sequences (ZC-seq) are used as preamble sequences, but the length of the sequence restricts the number of different sequences that can be generated. Especially for mMTC type communications where there is a very high density of connection requests, the probability of collision of preambles becomes higher, resulting in failure of RA procedure. The limited number of available preambles using ZC-seq create a need for other sequences to be studied that can provide more number of preambles which is result will reduce the reuse of a preamble and hence reduce the probability of collision.

The status of UE being in LoS or NLoS will highly impact the beam failure occurrence which initiates a fresh RA procedure. Thus the study of a UE going into NLOS state is important to know the signal quality it receives on average based on the path loss models. Using this information we can have a measure of beam failure probability. The RACH procedure uses resources, which can decrease the throughput. So the measurement of RACH success and failure also becomes important.

1.3 Approach

We divide our work into two parts. In the first part, we study the inherent properties of different preamble sequences and the effect of using different preambles on their detection performance. Second part consists of study of the mobility of an UE, obstacle density on the RACH success probability. We go through following steps to come to our results and conclusions:

1.3.1 Design and study of preambles and their performance

- Study the correlation properties of different candidate sequences for preamble generation.
- Propose a new candidate preamble sequence.
- Find their preamble capacity based on the inter-set and intra-set periodic correlation.
- Employ a detection algorithm to find out the detection probability for the considered preambles with respect to SNR. (while doing so we have to keep the false alarm probability $< 0.1\%$).
- Simulate different metrics like PAPR, CM for the sequences to be transmitted.

1.3.2 Study on the effect of mobility and obstacles on the Random Access Procedure

- Model UE mobility in a restricted area.
- Model the obstacles in 2-D geometry, based on the Poisson Point Process (PPP).

- Simulate the NLOS probability of UE based on its movement and obstalces.
- Based on the NLOS status, calculate the path-loss experienced by an UE and with this information calculate the beam-failure probability.
- Based on the the beam-failure recovery procedure,RACH instances, and path-loss for multiple UEs, employ the detection algorithm used in PART-I to detect the preambles and then find out the RACH success probability.

1.4 Aim of the work

The main goal of our work is to study the properties of the Zadoff-Chu, m, All-top and the proposed $mAll$ sequences considered to be the candidates for preamble generation, in attempt to suggest a sequence of higher preamble capacity to meet the demand of 5G, specifically mMTC type communication. Based on detection techniques find out their detection performance in AWGN channel and observe it effects on the detection-probability of the sequences. We also want to see the effect that equal gain combining has on the detection-performance of these sequences.

Secondly, we wish to find out the effects of speed, building density [1] on the RACH success probability, incorporating the detection-performance achieve in Part-I and to justify the results we see.

Thus we attempt to include both, PHY (Physical) layer performance and MAC (Media Access Control) layer performance metric to arrive at a total probability of RACH success.

[1] obstacle density and building density are used interchangeably

1.5 Outline Of Report

Chapter 1 gives a brief introduction for the motivation and background related to the project. In chapter 2 we discuss some theoretical concepts for preamble sequences, their periodic correlation and other properties.We give some background on the beam-management aspects. In chapter 3, we present the method used for simulation of results such as the PAPR, CM calculations, the detection method, mobility modelling, obstacle modelling and algorithms used for simulation . Chapter 4 has the record of all results simulated employing the algorithms discussed.

Chapter 2

Background

2.1 Literature Review

The preambles are generated on the principle of orthogonality between all different sequences between a set of sequences to identify a received preamble. Constant Amplitude Zero Auto Correlation (CAZAC) Sequences are considered to be suitable candidates for preamble generation. These sequences maintain Constant Amplitude so that the Peak to Average Power Ratio (PAPR) is low, which is required to maintain the linearity of Power Amplifiers. CAZAC sequences have another property, i.e. any two different sequences in a CAZAC sequence set are orthogonal to each other. ZC sequences have been used in LTE for preamble generation as they are CAZAC sequences. The length of a preamble sequence is based on the numerology defined by 3GPP technical specification. Here we have a sequence length $L = 839$ for FR1 band and $L = 139$ for FR2 band.Considering FR2 band use case for urban area, L = 139 is the chosen preamble length. This choice of preamble length limits the number of different preambles generated for a ZC sequence.

ZC sequences and its properties have been extensively studied in [3] [4]. ZC sequences are found to be sensitive to frequency shift. Another candidate sequence for preamble generation called m-Sequence is explored in [5] which shows better tolerance to frequency shifts. To increase the number of preambles available, several techniques were proposed in the literature. Aggregation techniques are explored in [6] where the transmitted preamble is a weighted addition of two ZC sequences. A new preamble is constructed in [7] by multiplying shifted versions of two different ZC sequences. The combination of ZC sequences with other CAZAC or near-CAZAC sequences has been suggested in [8], [9] .

The effect of diversity combining on the detection performance has not been explored in detail for these preamble sequences in particular in the literature. Furthermore, although PAPR properties of these sequences have been explored, Cubic Metric (CM), which is an important parameter, has not been studied for these sequences. This paper aims to find the detection performance using diversity combining of the proposed sequences and their CM measurements, which can help identify better overall sequences as candidates for preambles.

The study of mobility of a UE in given area is important. Different mobility models such as Manhattan model, Freeway model, Random Waypoint model are studied in [10]. A recurrent Gaussian mobility model is proposed in [11].The model in [11] accurately represents the movement of an UE in a restricted area. This model has both temporal and spatial dependence, which is closer to realistic movement of a UE. The propagation models and path loss models have been studied in [12], [13]. The working of beam pair formation has been studied in [14], [15]. However, to the best of our knowledge, the study of how the mobility of an UE affects the beam failure, how the building densities in an area affects it, how does the detection probability of preamble affect the collision and success probability of a RACH procedure.

2.2 PRACH- Physical Random Access Channel

In this section, we give a brief introduction as to how the number of preambles available for each of the cell are decided. We also give a brief introduction to the RACH procedure steps followed by UE and gNB to successfully complete the procedure.

2.2.1 Preamble Generation

For each cell there are 64 [1] preambles available at UE for transmission. N_{CS} value is obtained from higher layer parameter $zeroCorrelationZoneConfig$. Given the N_{CS} i.e. minimum cyclic shift, we can generate at most $\left\lfloor \frac{L_{RA}}{N_{CS}} \right\rfloor$ from a single root(μ). To generate 64 preambles, first the all cyclic shifts of a given logical root sequence are obtained in increasing order of C_v. If 64 preamble sequences cannot be generated from a single root index then next preamble are obtained from root sequences with consecutive logical root indexes[2] until all 64 preamble are generated. The starting logical root index is obtained from parameters such as $prach-RootSequenceIndex$. The UE chooses one of the preamble from the available 64 preamble randomly and initiates the RA procedure for up-link synchronisation and transmission.

2.2.2 Random Access Channel Procedure [RACH]

Random Access Channel Procedure is initiated by UE based on the information received through $SynchronisationSignalBlocks$ (SSBs), broadcasted by gNB. There are two types of RACH procedure i.e. $Contention-Based$ and $Contention-Free$. For $Contention-Free$ procedure there are reserved preambles so that there is no probability of collision in a RACH occasion. But for short preambles ($L_{RA} = 139$),

[1] This is valid for $L_{RA} = 139$. For $L_{RA} = 839$ there are restricted sets which limit the number of available preamble for transmission

[2] Root index of ZC sequence is mapped to logical root index as per [16]

there are no restricted sets, hence they go through $Contention - Based$ RACH procedure, which has following four steps:

- MSG-1: UE transmits preamble, based on the information acquired from SSBs such as time resources, frequency resources, preamble format, cyclic shifts.
- MSG-2: gNB after detecting the preamble sends Random Access Response (RAR) to UE.
- MSG-3: UE transmits PUSCH (Physical Up-link Shared Channel) to the same cell to which it transmitted its preamble. PUSCH carries different types of uplink control information. UE waits for gNB MSG-4 and starts $ContentionResolutionTimer$
- MSG-4: gNB transmits MSG-4 (Contention Resolution) to UE in PDCCH (Physical Down-link Control Channel). If the PDCCH is decoded successfully, the $ContentionResolutionTimer$ is stopped and RACH procedure is considered to be successfully completed.

Before going into details we present some formal definitions which are required throughout:

2.3 Definitions

2.3.1 Cyclic Shift

Let $x[n]$ be a sequence of length L, then the cyclic shifted $x_c[n]$ is defined as:

$$x^{n_0}[n] = x[(n + n_0)\ mod\ L] \tag{2.3.1}$$

2.3.2 Periodic Correlation

Periodic correlation of any two sequences $x[n]$ and $y[n]$ of length L is given by following

$$R_{x,y}[\tau] = \sum_{n=0}^{L-1} x[n]y^*[(n+\tau)\ mod\ L)] \tag{2.3.2}$$

2.3.3 Power Delay Profile (PDP)

PDP is calculated as following:

$$P_{x,y}[\tau] = |R_{x,y}[\tau]|^2 \tag{2.3.3}$$

where $R_{x,y}[\tau]$ is defined in Eq. (2.3.2)

2.3.4 Diversity Combining

Equal gain combining is a simpler combining technique where we use signals obtained from different antennas and add them directly for further processing. So for N_{Ant} number of receiver antennas at gNB, after equal gain combining of the PDPs we have:

$$P^i_{N_{Ant}} = \sum_{l=1}^{l=N_{Ant}} P^i_l \tag{2.3.4}$$

2.3.5 Zero/Low Correlation Zone (ZCZ)/(LCZ)

Considering the value obtained in Eq. (2.3.3), the ZCZ/LCZ is defined as the region of values of τ where the value of $|P_{x,y}[\tau]|$ is zero/very low as compared to the peak value $|P^{max}_{x,y}|$

2.3.6 Probability of Detection/Misdetection

$P(detection)$ is defined as the conditional probability of correct detection of the preamble when the signal is present. $P(miss)$ is complementary of $P(detection)$. $P(detection)$ should be equal to or exceed 99%.The error cases for $P(detection)$ are:

- Detecting different preamble than the one that was sent
- Not detecting the preamble at all
- Correct detection with wrong timing estimates

2.3.7 Probability of False Alarm

$P(false)$ is defined as the conditional probability of erroneous detection of the preamble when input is noise only. $P(false)$ should be less than 0.1%[3].

For all further discussion we consider length of preamble $L = L_{RA}$ =139.

2.3.8 Preamble Capacity ($PrCapacity$)

Preamble Capacity of a sequence can be defined as the total number of unambiguous sequences that can be generated from a candidate CAZAC or near-CAZAC sequences.

2.4 PAPR and Cubic Metric

PAPR and CM are the metrics which indicate the efficiency of Power Amplifier(PA) used to transmit the signals.Generally, higher the PAPR or CM, the efficiency of

[3]The conditions on $P(miss)$ and $P(false)$ for different channels are defined in 3GPP TS 38.104 V16.4.0

the PA will be lower. PAPR gives us the measure of power backoff required. For a transmitted signal $x(t)$ PAPR is define by:

$$PAPR[x(t)]dB = 10\log\frac{max[x^2(t)]}{mean[x^2(t)]} \tag{2.4.1}$$

However, recent studies suggest that the CM is a better predictor than the PAPR metric [17] [18] [19] as it considers the effect of 3rd order harmonics introduced due to the non-linearity in PA. In general the amplifier voltage can be written as :

$$v_0(t) = g_1 v_i(t) + g_3 v_i^3(t) \tag{2.4.2}$$

where g_1 and g_3 are linear and non-linear gains respectively. These gains are inherent to PAs and do not change with the type of signal. The cubic term in Eq. (2.4.2) introduces distortions in the transmitted signal, resulting in erroneous detection at receiver, moreover it also introduces third harmonics which interfere with adjacent channels. In order to suppress these distortion we need to suppress the non-linear gain (g_3). The CM for a transmitted signal $x(t)$ is given by:

$$\begin{aligned} CM[x(t)] &= \frac{20\log rms[x^3_{norm}(t)] - 1.52}{1.56} \\ where \quad x_{norm}(t) &= \frac{\text{mod } x(t)}{rms[x(t)]} \end{aligned} \tag{2.4.3}$$

2.5 CAZAC sequences

CAZAC sequences is short for Constant Amplitude Zero Auto-Correlation sequences. As the name implies these sequences have following properties:

For a given complex-valued periodic sequence $x[n]$ of length L_{RA}

1. $|x[n]| = 1 \quad \forall n$

2. $R_{x,x}[\tau] = 0 \quad for \quad \tau \neq 0$

The 1^{st} property i.e. constant amplitude property of CAZAC is desirable for lower PAPR and 2^{nd} property is useful for identification of signal. Lets explore 2^{nd} property in more detail. For a given CAZC sequence $x[n]$ and its cyclic shifted version $x^{n_0}[n]$ defined in Eq. (2.3.1), consider its PDP in Eq. (2.3.3), we have:

$$\begin{aligned} P_{x,x^{n_0}}[\tau] &= 0 \quad for \quad \tau \neq n_0 \\ P_{x,x^{n_0}}[\tau] &= max \quad at \quad \tau = n_0 \end{aligned} \tag{2.5.1}$$

From Eq. (2.5.1), it is clear that a cyclic shifted version of a CAZAC sequence can be detected based on the index of maximum value obtained. Thus we deduce:

- For a same sequence, we are able to detect if the sequence received is a cyclic shifted version of the sequence or not and the extent of cyclic shift.
- The sequence $x[n]$ and $x^{n_0}[n]$ are orthogonal to each other considering the fact that $P_{x,x^{n_0}}[\tau] = 0$ for $\tau = 0$, meaning their inner product is zero.

.This property becomes very useful for development of set of preambles used for transmission. Let for a sequence $x[n]$ there are restrictions on cyclic shift that we can only generate cyclic shifts of sequence with integer multiple of N_{CS} defined as C_v such that:

$$C_v = vN_{CS}, \quad v = 0, 1, ..., \left\lfloor \frac{L_{RA}}{N_{CS}} \right\rfloor \tag{2.5.2}$$

i.e only allowed value of n_0 in Eq. (2.3.1) are $0, N_{CS}, 2N_{CS}, ..., \left\lfloor \frac{L_{RA}}{N_{CS}} \right\rfloor N_{CS}$, then we can say that for a given CAZAC sequence $x[n]$ we have a total of $\left\lfloor \frac{L_{RA}}{N_{CS}} \right\rfloor$ orthogonal sequences present, which can be detected unambiguously. We define such set of

orthogonal cyclic shifted sequences as:

$$\mathfrak{s}_x^{CS} = \bigcup_{v=0}^{\left\lfloor \frac{L_{RA}}{N_{CS}} \right\rfloor} x^{C_v}[n] \qquad (2.5.3)$$
$$where \quad x^{C_v}[n] = x[(n + C_v)\ mod\ L_{RA}]$$

If we have other CAZAC sequences namely $w[n], y[n], z[n]$ and so on, which can form similar sets as defined in Eq. (2.5.3) and also if the sequences $w[n], x[n], y[n], z[n]$ are mutually orthogonal or have very low cross-correlation, we can form a super-set of sequences such that:

$$\mathfrak{S}_{w,x,y,z}^{CS} = \{\mathfrak{s}_w^{CS}, \mathfrak{s}_x^{CS}, \mathfrak{s}_y^{CS}, \mathfrak{s}_z^{CS}\} \qquad (2.5.4)$$

For such different N number of sequences where each of the sequences is a CAZAC sequence limited by C_v, and zero or low cross-correlation we can derive the total number of sequences in super-set as:

$$Total\ number\ of\ sequences = N \times \left\lfloor \frac{L_{RA}}{N_{CS}} \right\rfloor \qquad (2.5.5)$$

where, each sequence can be detected and there is no similarity between any two sequence. Such a set of sequence is very useful for preamble generation because each of the sequence can be used by different users to identify themselves in the system. With this said, we look into the properties of Zadoff-Chu (ZC) sequences and build on to what we saw in this section.

2.6 Zadoff-Chu sequences (ZC)

ZC-seq is defined as:

$$x_\mu[n] = \exp^{-j\frac{\pi\mu n(n+1)}{L_{RA}}}, \quad \begin{aligned} 0 \leq n \leq L_{RA} - 1 \\ 1 \leq \mu \leq L_{RA} - 1 \end{aligned} \tag{2.6.1}$$

where μ is the root of the ZC sequence which is relatively prime to L_{RA}. As $L_{RA} = 139$ which is a prime number,all values of μ varying from 1 to $L_{RA} - 1$ are valid. Therefore, we have $N_{ZC} = L_{RA} - 1$ different root sequences. Some properties of ZC sequences are:

- The ZC sequence with a given root is orthogonal to all its cyclic shifted versions. Therefore, the periodic auto-correlation and PDP defined in Eq. (2.3.2) (2.3.3)of a ZC seq with its cyclic shifted version is zero for the same root i.e.

$$R_{x,x^{n_0}} = 0, \quad n_0 \neq 0 \tag{2.6.2}$$

- The periodic auto-correlation of two ZC sequences with different roots is low and constant i.e.

$$R_{x_\mu, x_{\mu'}} = \sqrt{L_{RA}} \tag{2.6.3}$$

Different cyclic shifted version of a ZC sequence of the same root μ can be obtained as:

$$x_\mu^v = x_\mu[(n + C_v)\ mod\ L_{RA}] \tag{2.6.4}$$

where C_v correspond to a cyclic shift defined by

$$C_v = \begin{cases} vN_{CS}, & v = 0, 1, ..., \lfloor \frac{L_{RA}}{N_{CS}} \rfloor,\ N_{CS} \neq 0 \\ 0, & N_{CS} = 0 \end{cases} \tag{2.6.5}$$

where N_{CS} is the minimum cyclic shift allowed which is dependent on cell radius R, L_{RA}, maximum delay spread τ_{max}, time required to transmit the sequence T_{seq}, speed of light c_0 and n_g are additional guard samples:

$$N_{CS} > \left\lceil \left(\frac{2R}{c_0} + \tau_{max} \right) . \frac{L_{RA}}{T_{seq}} + n_g \right\rceil \tag{2.6.6}$$

2.6.1 Preamble capacity of ZC sequence ($PrCapacity^{ZC}$)

We know that μ varies between 1 to $L_{RA} - 1$. Therefore we have $N = L_R A - 1$ different sequences which have very low cross-correlation. Using the definition given in Eq. (2.5.5) we have:

$$PrCapacity^{ZC} = (L_{RA} - 1) \left\lfloor \frac{L_{RA}}{N_{CS}} \right\rfloor \tag{2.6.7}$$

Limitations:

We now see that for $L_{RA} = 139$, we have very limited number of preambles at our disposal based on N_{CS}. The value of $N_C S$ is defined in [16] by a $zeroCorrelationZoneConfig$ parameter given in Table 2.1:

Considering Test case preambles defined in [20], considering a $N_{CS} = 23$, we have $138 \times \lfloor 139/23 \rfloor = 828$ different sequences only. This may cause a reuse of preamble sequence in neighbouring cell, which may lead to severe interference and collisions. To avoid this we wish to have sequences with high preamble capacity.

We will talk in detail about the method used for preamble detection is coming chapters.

Next, we look at some Beam-Management aspects which guide us to the simulation procedure we follow.

$zeroCorrelationZoneConfig$	N_{CS}
0	0
1	2
2	4
3	6
4	8
5	10
6	12
7	13
8	15
9	17
10	19
11	23
12	27
13	34
14	46
15	69

Table 2.1: N_{CS} with preamble format $L_{RA} = 139$

2.7 Beam Management

The main difference in RACH procedure for LTE and 5G NR is Beam Alignment. For a UE to transmit a preamble sequence first beam alignment is necessary, especially for mmWave. As mmWaves are transmitted using antenna arrays, which then use multiple antenna elements to direct the beam in a particular direction. Giordani *et al.* [14], Li *et al.* [15] give us the introduction about the aspects of beam management. Beam Management can be defined as the procedure required to trace-out a set of beam pair links between UE and gNB and maintain them throughout. Beam Management procedure consists of following steps which help for beam-forming:

1. Beam Sweeping
2. Beam Measurement

3. Beam Reporting
4. Beam Determination
5. Beam Maintenance
6. Beam Failure Recovery

2.7.1 Beam Forming Aspects

We take a look at each of the steps mentioned above and their functions.

Beam Sweeping

As the name suggest, the beams of transmitter and receiver sweep in every direction to cover a spatial area in a determined way. For example, when transmitting SSB, the gNB sweeps acrross spatial area and transmits in bursts. These SSB bursts last for $5ms$ and their default periodicity is $20ms$. Whereas, the UE also sweeps beams spatially to receive the best beam.

Beam Measurement

The UE and gNB selects the best beam based on the the Reference Signals. There are two cases for measurements:

- **Based on CSI-RS:** This is done at downlink. The UE after receiving CSI-RS(Channel State Information- Reference Signal) resources, performs measurements such as Beam-ID corresponding the CSI-RS resource, Reference Signal Received Power(RSRP) and report it back to gNB.
- **Based on SRS:** UE transmitts SRS (Sounding Reference Signal) to the gNB. Beam selection is done at gNB after measurement of SRS. The beam at which

maximum received power is detected is selected thus the angle of arrival of signal and angle of departure is decided by gNB.

Beam Reporting

Beam reporting corresponds to the reporting of information of the BeamFormed signal recevied based on the Beam Measurements.The measurement quantity that an UE can report is RSRP. There are two types of reporting:

- **Group Based:** UE can enables multiple antenna elements to receive signal from gNB, for different paths. Thus UE helps the gNB to identify mutliple paths which are observed by the UE and lets the gNB take further actions based on the information reported.
- **Non-Group Based:** UE reports only one of the best beams measured by it to the gNB. Therefore gNB can transmit on only one beam after receiving the information.

Beam Determination

The gNB after receiving the information from UE in the previous step, it decides to select the best beam for data transmission.

Beam Maintenance

Beam Maintenance includes beam tracking and refinement. After initial beam selection, the gNB and UE may opt for beam refinement in order to get highly directional beam for higher data rates. This is referred to as beam refinement. Beam tracking is useful when we have a mobile UE. This is done by probing neighbouring beam and continuously tracking the neighbouring beam in groups so as to compensate change for optimal transmission.

Beam Failure Recovery

The directional beams introduce higher data rates but also are very sensitive to channel fluctuations. A N-LOS condition can cause the signal to degrade severely as compared to LOS condition. Beam failure occurs when the beam maintenance fails to properly track the beams. UE may experience fast shadowing as mentioned or beam switching procedure may fail. Beam failure can be declared based on measurement filtering threshold (indicating quality of signal) or a timer when doing beam switching. It is important to note that at each Beam Failure instance RACH procedure is initiated by UE for up-link establishment.

Chapter 3

Candidate sequences

In this chapter, we look at candidate preamble sequences proposed in literature and we propose a new candidate sequence with even higher preamble capacity.

3.1 Concept of cover sequences

From (2.6.7) we have a fixed number of preamble sequences that can be generated based on L_{RA} and N_{CS}. Lets denote this set of sequences as S^{ZC}. Consider another sequence $c[n]$ of length L_{RA}. Assuming we can generate N_c number of sequences from $c[n]$ which are all orthogonal or non-ambiguous to one another. We can define this set of N_c sequences as S^c. Here non-ambiguity implies that the cross-correlation between any two sequences from the set is very low so that they can be identified and detected easily. We can make use of the sequences in S^c as cover sequences.

Cover sequence implies that each sequence from S^c multiplies each sequence from

S^{ZC} element-wise. Therefore we have

$$S^c = \{c_1[n], c_2[n], c_3[n], \ldots, c_{N_c}[n]\} \tag{3.1.1}$$

We define the new sequence obtained from applying the cover sequences as $y[n]$

$$\begin{aligned} y[n] = c_l[n].*x_\mu^v[n], \quad & l = 1, 2, \ldots, N_c \\ & \mu = 1, 2, \ldots, L_{RA} - 1 \\ & v = 0, 1, \ldots, \lfloor \frac{L_{RA}}{N_{CS}} \rfloor \\ & n = 0, 1, \ldots, L_{RA} - 1 \end{aligned} \tag{3.1.2}$$

Here in (3.1.2), ".$*$" represents element-wise multiplication. For each cover sequence $c_l[n]$, we have a set of sequences defined in (2.6.7) defined as S_l^{ZC}. We will have a union of all such N_c sets as our final set S^{cZC}

$$S^{cZC} = \bigcup_{l=1}^{N_c} S_l^{ZC} \tag{3.1.3}$$

Popovic in [21] defines such set in (3.1.3) as Quasi-Orthogonal Set.

3.2 $m-sequence$ and combination with ZC sequence(mZC)

$m-sequences$ are binary sequences generated by using Linear Feedback Shift Registers (LFSR) [5] [9]. Generation of these sequences are define by its primitive

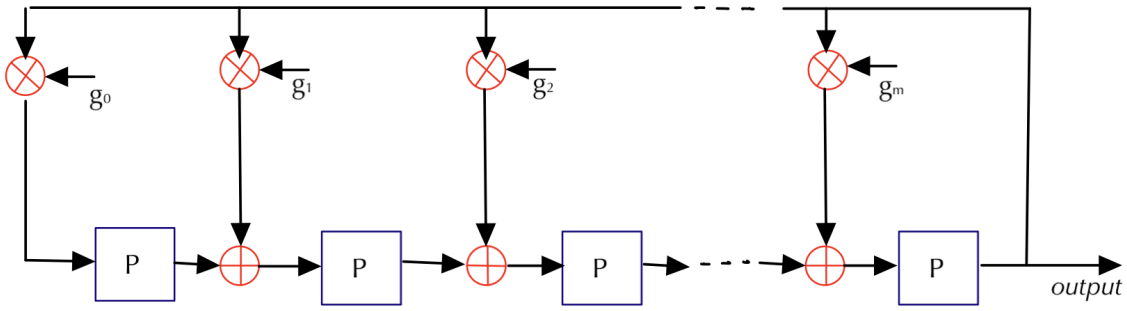

Figure 3.1: $m-sequence$ generator

generator polynomials.A m^{th} order polynomial is defined as :

$$g(P) = g_m P^m + g_{m-1} P^{m-1} + \cdots + g_1 P^1 + g_0 \tag{3.2.1}$$

The length of sequence is given by $N_m = 2^m - 1$. For example consider $m = 7$, we have a length of sequence as $N_m = 127$ and generator polynomial as $P^7 + P^1 + 1$. Using these polynomial weights, LFSRs will generate a periodic binary bit streams $x_m[n]$of length 127.

We can obtain a set of orthogonal sequences S^m from $x_m[n]$ by cyclic shifting the sequences.

$$x_m^{n_0}[n] = x_m[(n + n_0)\ mod\ L] \tag{3.2.2}$$

$$S^m = \bigcup_{n_0=0}^{N_m-1} x_m^{n_0}[n] \tag{3.2.3}$$

The inherent issue with the m-sequences is that they are defined perfectly for lengths of $2^m - 1$ i.e 3, 7, 15, 31, 63, 127, 255, 511 and so on. As define by 3GPP Technical specifications, the length for short preamble is defined as $L_{RA} = 139$. The closest length for $m - sequence$ is 127 i.e. $m = 7$. At the defined lengths the cyclic shifted versions of $m - sequences$ defined in (3.2.2) are orthogonal to each other. But the need of sequences length of 139 arises an issue. For this we simply extend

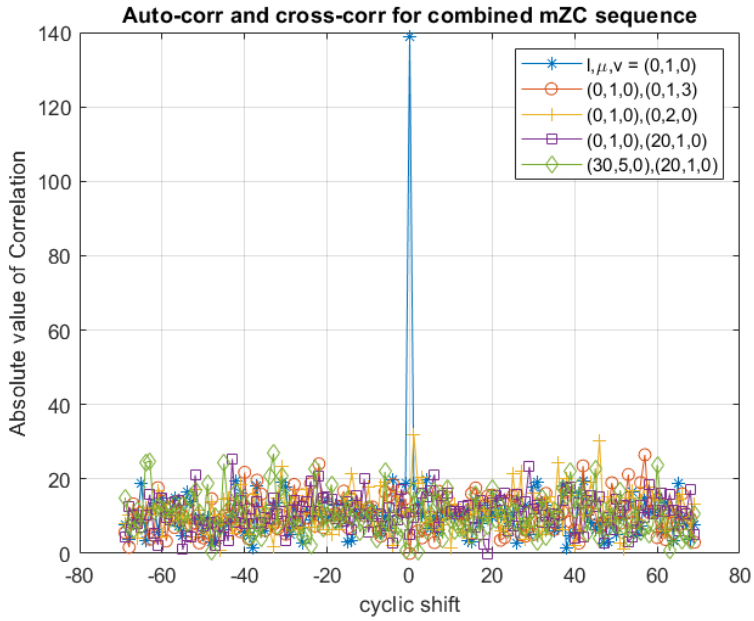

Figure 3.2: Periodic Correlation of mZC sequences

the $m-sequences$ to be generated for the length of 139 such that we append the first 12 samples of $m-sequence$ to itself thus creating a desired length sequence. Although the new sequences generated lose their orthogonality, but all the sequences maintain their non-ambiguity and their cross-correlation is very low compared to the total energy of signal. They behave as near-CAZAC sequences.

From 3.1, we can use the $m-sequences$ as a cover sequence to obtain a Quasi-Orthogonal set S^{mZC} [9] from (3.2.4) as below:

$$z_{l,\mu,v} = x_m^{n_0}[n].*x_\mu^v[n]) \tag{3.2.4}$$

To check for how many preamble sequences can be obtained from using $m-sequences$ as cover we see that we can use the set S^{ZC} as it is. Then we have N_m number of sequences in set S^m. Therefore multiplying each sequences in S^m with each sequence in S^{ZC} we will have $N_m(L_{RA}-1)\left\lfloor\frac{L_{RA}}{N_{CS}}\right\rfloor$ sequences along with the

original ZC set. Therefore we have

$$\begin{aligned} PrCapacity^{mZC} &= N_m(L_{RA}-1)\left\lfloor\frac{L_{RA}}{N_{CS}}\right\rfloor \\ &\quad + (L_{RA}-1)\left\lfloor\frac{L_{RA}}{N_{CS}}\right\rfloor \\ &= (N_m+1)(L_{RA}-1)\left\lfloor\frac{L_{RA}}{N_{CS}}\right\rfloor \end{aligned} \tag{3.2.5}$$

From Fig. 3.2, we verify the correlation properties of mZC sequences formed in (3.2.4). We change the parameters l, μ, v and check for different combination to verify that the periodic auto-correlation gives us a peak at centre, but cross-correlation yield very low values at all locations. This leads to unambiguous signal detection.

3.3 *AllTop* and combination with ZC sequence(aZC)

AllTops's sequences are define in [22] as cubic phase sequences. One form of such sequences are defined in [9] [23] as follows:

$$\begin{aligned} a_{\lambda,w}[n] = \exp -j2\pi\frac{(n+w)^3+\lambda n}{L_{RA}}, \quad & 0 \le n \le L_{RA}-1 \\ & 0 \le \lambda \le L_{RA-1} \\ & 0 \le w \le L_{RA-1} \end{aligned} \tag{3.3.1}$$

Some properties:

- $a_{\lambda,w}[n]$ is a cyclic shifted version of the sequence $a_\lambda[n]$, where $w = 0$.
- Two sequences $a_{\lambda,w}[n]$ and $a_{\lambda',w}[n]$ are orthogonal to each other.
- Whereas, $a_{\lambda,w}[n]$ $a_{\lambda,w'}[n]$ have very low cross correlation i.e equal to $\sqrt{L_{RA}}$.

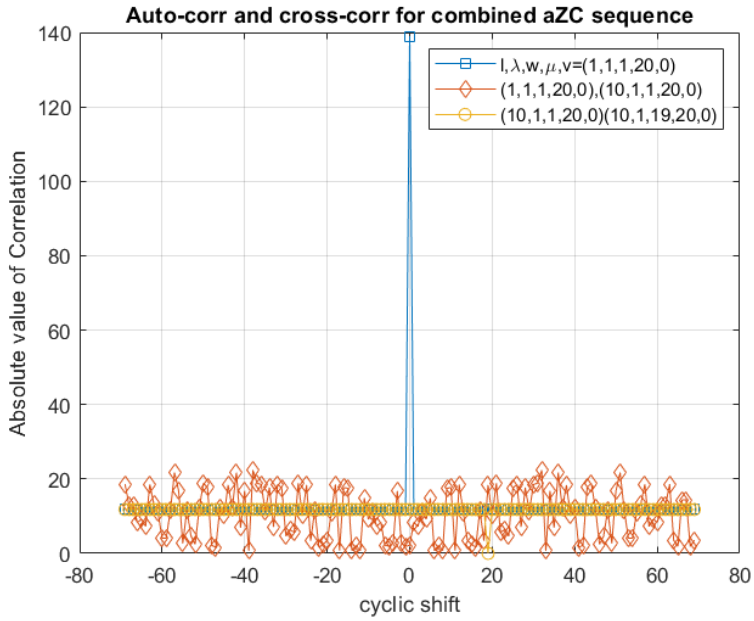

Figure 3.3: Periodic Correlation of aZC sequences

Applying the sequence in (3.3.1) as a cover to ZC-sequence introduces ambiguity in resulting sequences. Pitaval *et al.* in [9] discusses this in details and proposes a new cover sequence to be used as:

$$z_{l,\lambda,w,\mu,v} = (a_{\lambda,w}[n])^{l} . * x_{\mu}^{v}[n] \tag{3.3.2}$$

This results into Preamble capacity of

$$PrCapacity^{aZC} = \left(L_{RA}^{2} - 1\right) \left\lfloor \frac{L_{RA}}{N_{CS}} \right\rfloor \tag{3.3.3}$$

Fig.3.3 show the periodic correlation results for different combinations of values of l, λ, w, μ, v. For same signal we observe that the peak occurs at centre, but then for other lag values we have LCZ. Keeping the ZC root sequence same but changing

the l value result in non-closed form result but it is lower compared to peak value hence can be considered as LCZ. Keeping the ZC root sequence and l same but cyclic shifting All-top sequence by w=19, result in orthogonality at 19th location, but other than that, it remains in LCZ.We cannot use all different combinations of the values l, λ, w, μ, v to generate preambles, because there could be ambiguity in some of the combinations. Hence the limit given in (3.3.3).

3.4 Combination of m and AllTop sequences (mALL)

We propose a new combination sequence while using m-sequence as a cover sequence for AllTop sequence. Therefore, from (3.3.1),(3.2.2), we have :

$$z_{l,\lambda,w,t} = \left(a_{\lambda,w}[n]\right)^{l} . * x_{m}^{t}[n] \tag{3.4.1}$$

Fig. 3.4 shows the correlation results for different combinations of $l,\ w, t$. The maximum LCZ value in this case is $\leq 3\sqrt{L_{RA}}$. Motivation behind considering an combination of m and AllTop sequences is the reason that in [9] is has been argued that the combination of AllTop and ZC sequence may arise some ambiguity in sequences for any arbitrary cyclic shifts. This can be avoided with the use of m sequences instead of ZC sequences.From exhaustive search by varying parameters and periodic-correlations, we observe that:

- For $z_{l,\lambda,w,t}$in (3.4.1), each different l produces a LOW correlation sequence.
- Each λ also produces LOW correlation sequences.
- Each change in w also produces LOW correlation sequences for a fixed t
- For different values of t, we face ambiguity in the sequences and it results in high correlation peak.

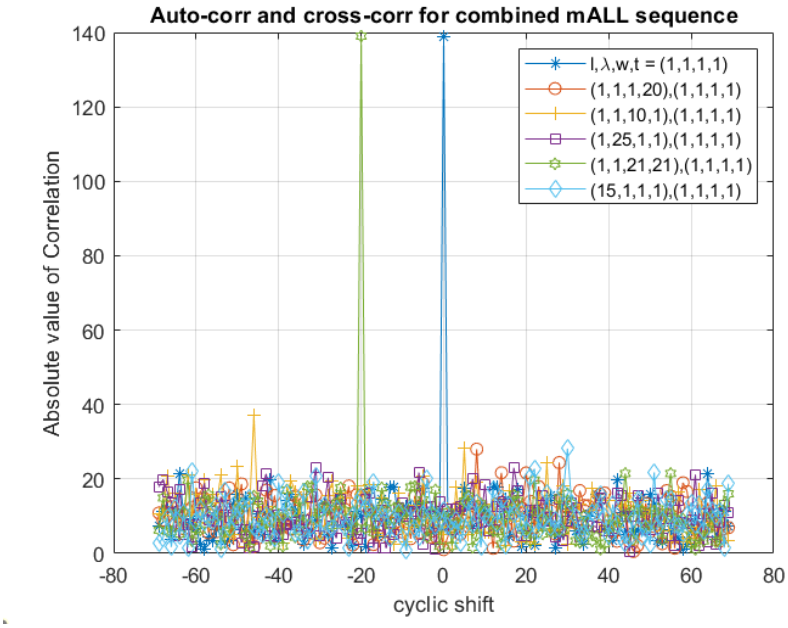

Figure 3.4: Periodic Correlation of $mALL$ sequences

So each sequence we get from above information will be unambiguous. For a fixed value of l, λ, w, t, we introduce a new parameter v such that

$$z^{v}_{l,\lambda,w,t} = z_{l,\lambda,w,t}[(n + C_v)\ mod\ L_{RA}] \\ C_v\ is\ defined\ by\ Eq.(2.6.5) \tag{3.4.2}$$

Lets define a set of such sequence as:

$$s^{mALL} = \bigcup_{v=0}^{\left\lfloor \frac{L_{RA}}{N_{CS}} \right\rfloor} z^{v}_{l,\lambda,w,t}[n] \tag{3.4.3}$$

From (3.4.3), we get $\left\lfloor \frac{L_{RA}}{N_{CS}} \right\rfloor$ sequences. Combination of all such set will form a complete set such that:

$$
\begin{aligned}
S^{mALL} &= \bigcup_{l,\lambda,w,t} s^{mALL} \\
0 &\leq l \leq L_{RA} - 1 \\
0 &\leq \lambda \leq L_{RA} - 1 \\
0 &\leq w \leq L_{RA} - 1
\end{aligned}
\tag{3.4.4}
$$

Taking all combinations into account we can calculate PRACH capacity for the proposed sequence:

$$
\begin{aligned}
PrCapacity^{mALL} &= L_{RA} \times L_{RA} \times L_{RA} \times \left\lfloor \frac{L_{RA}}{N_{CS}} \right\rfloor \\
&= L_{RA}^{3} \left\lfloor \frac{L_{RA}}{N_{CS}} \right\rfloor
\end{aligned}
\tag{3.4.5}
$$

We see from (3.4.5),the proposed $mALL$ sequence has a much larger $PrCapacity$ than the previous identified sequences namely ZC, mZC and aZC.

Chapter 4

System Model and Simulation Procedures

4.1 Preamble Detection

gNB has the information about which root sequences are present in all 64 preamble from which UE transmits one of the preamble randomly. To calculate the periodic correlation we make use of FFT for faster calulations. As we know the convolution of two sequences in time domain is equivalent to the operation of element wise multiplication of the FFT of sequences.Let the received sequence be $s[n]$ and the root sequences present at gNB be $k_\mu[n]$.

$$\mathcal{F}(s[n]) = S[k] \quad \mathcal{F}(k_\mu[n]) = K_\mu[n] \tag{4.1.1}$$

$$\begin{aligned} R_{s,k_\mu}[\tau] &= \sum_{n=0}^{L-1} s[n]k_\mu^*[(n+\tau)\ mod\ L)] \\ &= \mathcal{F}^{-1}(K_\mu^*[n].S[k]) \end{aligned} \tag{4.1.2}$$

4.1.1 Preamble Detection Algorithm

The detection algorithm is implemented as follows:

- Calculate $FFTs$ of received sequence $s[n]$ and $k_\mu[n]$
- Using (4.1.2) calculate the periodic correlation.Let $R^i_{s,k_\mu}[\tau]$ be the i^{th} correlation results corresponding to each root sequence.
- Calculate the Power Delay Profile (PDP) of each result, as:

$$P^i = |R^i_{s,k_\mu}[\tau]|^2 \tag{4.1.3}$$

- Accumulate the obtained PDP in (4.1.3) from all antennas non-coherently using equal gain combining technique Eq. (2.3.4)
- Calculate Threshold η from Eq.(4.1.4), (4.1.5) for detection of preamble.
- Divide the PDPs obtained from (4.1.5) into a windows of length N_{CS} defined by $zeroCorrelationZoneConfig$.
- In each window for every sample check for the peak value. If the peak value is greater than η then the corresponding preamble is detected.

4.1.2 Threshold Measurement

Each of the PDP obtained from (2.3.4) is normalised by its average value $\overline{P^i_{N_{Ant}}}$.

$$\overline{P^i_{N_{Ant}}} = \frac{1}{L_{RA}} \sum_{l=0}^{l=L_{RA}-1} P^i_{N_{Ant}} \tag{4.1.4}$$

Therefore from (2.3.4) and (4.1.4) we have normalised PDP

$$P^i_{Norm} = \frac{P^i_{N_{Ant}}}{\overline{P^i_{N_{Ant}}}} \tag{4.1.5}$$

Compare the value obtained in (4.1.5) with a decided value of η. If the value is greater, then preamble is detected else not.

The value of η is decided such that the condition for $P(false)$ defined in 2.3.7 is satisfied.

4.2 Simulating CDF of CM and PAPR

Simulations of CDF od CM and PAPR for the sequences have been done.

- For ZC sequence we set $zeroCorrelationZoneConfig$ =11, which translates to $N_{CS} = 23$ and $L_{RA} = 139$. From (2.6.7), we have 828 different sequence.
- For mZC, in (3.2.5) consider m-seq with cyclic shifts of 2 units. This results in $N_m = 70$ different M-sequences. So in total we have, 58788 different sequences.
- For aZC, from (3.3.3), similar to mZC we generate 57960 different sequence.
- For $mALL$ sequence we limit our sequences to lower number of sequences i.e. 57960 due to simulation constraints.

We simulate PAPR and CM measurements in following steps:

- Considering time domain sequences defined in (2.6.1),(3.2.4) and (3.3.2), (3.4.1) calculate its FFT of length 139 to convert them into frequency domain.
- Map these to 4096 sub-carriers to be generated as OFDM symbols and take IFFT to form time domain signal.
- Add the cyclic-prefix (CP) of length 288 which will give us the final time domain signal to be transmitted.
- Based on the transmitted time signal obtain the CDF for PAPR and CM using (2.4.1) and (2.4.3).

4.3 Gauss-Markov Mobility Model and Obstacle Modelling

To model the movement of a UE in an area we use Gauss-Markov mobility model with some modification decsribed in [11]. We decide to use this model over other models like Manhattan or Freeway model because the movement pattern is restricted in such cases. Where as Gauss-Markov mobility model has a temporal dependence which can mimic a random and continuous movement of an UE in open area.For iterating over many instances it has a possibility of covering all possible conditions. For our model we wish to restrict the mobility of UE in a given area hence we make a partial use of model defined in [11] which defines Gauss-Markov Mobility as follows:

$$\begin{aligned} S_{t+1} &= \alpha S_t + (1-\alpha)\overline{S} + \sqrt{1-\alpha^2}\mathcal{N}(0,1) \\ D_{t+1} &= \alpha D_t + (1-\alpha)\overline{D} + \sqrt{1-\alpha^2}\mathcal{N}(0,1) \end{aligned} \tag{4.3.1}$$

Parameters	**Values**
α	0.1 to 0.9
$\overline{S}$	1 to 10 m/s
S_t(initial speed)	$\mathcal{U}$[0,1]*$\overline{S}$
D_t(initial direction)	$\mathcal{U}$[0,2π]
x_t,y_t	$\mathcal{U}$[-250,250]
Size of buildings	$\mathcal{U}$[10,30] meters
Location of buildings	$\mathcal{U}$[-250,250]
Instances	10000

Table 4.1: Mobility Parameters

where S_{t+1} and D_{t+1} represent speed and direction at next instance, $\overline{S}$ and $\overline{D}$ are mean speed and direction, α is tuning parameter and $\mathcal{N}(0,1)$ is Standard Normal Random Variable. Based on (4.3.1) we define next position of UE as:

$$\begin{aligned} x_{t+1} &= x_t + S_{t+1} cos(Dt+1) \\ y_{t+1} &= y_t + S_{t+1} sin(Dt+1) \end{aligned} \tag{4.3.2}$$

Note that for $\alpha = 0$, the mobility model loses its dependence on previous speed in (4.3.1), which we do not want. We want a dependence on the previous speed for realistic observation. For $\alpha = 1$, the speed and direction become constant, which looses its randomness, which we wish to be present for our modelling.

We generate obstacles, such that the number of obstacles are generated using Poison Point Process (PPP) and then obstacles are placed uniformly across the area near gNB. Fig.4.1 shows the path traced by UE. It mimics the continuous path that can be taken by a UE. Obstacles represent buildings in the area.

For,simulation of UE mobility we use the parameters given in Table 4.1.We consider a square area of dimensions 500×500 meters, in 2-D considering the top view of the area. gNB is located at origin of the map. We consider a pedestrian/ve-

hicular scenario,assumption being made that the UE is outside the buildings. All simulations have been done using MATLAB. Steps followed in the simulations are:

- For each iteration, model the mobility of UE using (4.3.1) (4.3.2) for 10,000 instances and obstacles using PPP.
- For each instance, determine the status of UE i.e. LOS or N-LOS described in Section 4.4
- Depending on the status of UE and find the path-loss for every instance described in Section 4.5
- Simulate above steps for 1000 iterations to arrive at the P(N-LOS) and probability of beam failure.

4.4 Non-Line of Sight (N-LOS)

For a N-LOS condition to occur, there must be no direct path from the position of UE to gNB. This can occur when the UE is behind a certain obstacle, with respect to gNB. Using Table 4.1 we choose size of each building uniformly and form a square to represent it. Considering the quadrant in which an obstacle lies we decide two corner points and calculate their angles and distance from origin. If at any instance UE lies beyond the measured distance of obstacle and in between the angles, then N-LOS is declared.

4.5 Beam-Failure

Beam Failure may occur due to fast shadowing experienced by UE or while beam-switching. Beam Failure is essential to account for RACH procedure performance as

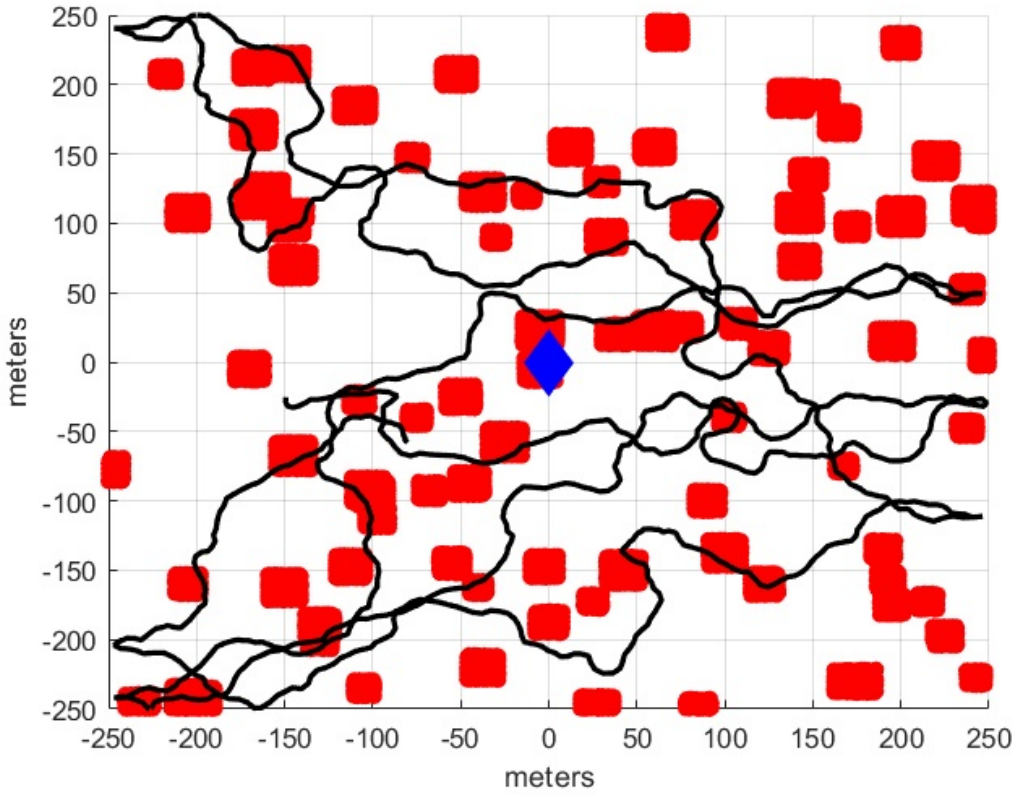

Figure 4.1: UE tracing the path using Gauss-Markov mobility and obstacle distributions

Variables	**Values**
h_{UT}	1.5 meters
h_{BS}	25 meters
f	30×10^9 Hz
f_c	30 GHz normalised with 1 GHz
Ω	120 dB

Table 4.2: Mobility Parameters

RA occasion is triggered when beam failure occurs. For Beam-Failure to be declared following condition have to be satisfied:

- The path-loss experienced by UE at any instance in accordance with Fig.4.2 defined in [2] should be greater than a set threshold value Ω.
- The UE should remain in above condition for two or more instances, such that the MAC counter is exhausted.

In Fig.4.2, d_{2D} is the distance from base of gNB to base of UE. d_{3D} is the distance of UE from antenna of gNB.h_{UT} and h_{BS} are height of UE and gNB respectively. σ_{SF} represents the standard deviation of shadow fading. When calculating path loss we also have to take into account the shadow fading of the channel in order to accurately estimate the total path loss.

$$d_{3D} = \sqrt{d_{2D}^2 + (h_{BS} - h_{UT})^2}, \quad 1.5m \leq h_{UT} \leq 22.5m \tag{4.5.1}$$

$$d_{BP} = \frac{4h_{BS}h_{UT}f}{c} \tag{4.5.2}$$

UMa	**LOS**	$\boldsymbol{PL_{UMa-LOS}} = \begin{cases} PL_1 & for\ 10m \le d_{2D} \le d'_{BP} \\ PL_2 & for\ d'_{BP} \le d_{2D} \le 5\ km \end{cases}$ $PL_1 = 28.0 + 22\log_{10}(d_{3D}) + 20\log_{10}(f_c)$ $PL_2 = 28.0 + 40\log_{10}(d_{3D}) + 20\log_{10}(f_c) - 9\log_{10}[(d'_{BP})^2 + (h_{BS} - h_{UR})^2]$	$\boldsymbol{\sigma_{SF} = 4}$
	NLOS	$\boldsymbol{PL_{UMa-NLOS}} = \max(PL_{UMa-LOS}, PL'_{UMa-NLOS})$ $for 10m \le d_{2D} \le 5km$ $PL'_{UMa-NLOS} = 13.54 + 39.08\log_{10}(d_{3D}) + 20\log_{10}(f_c) - 0.6(h_{UT} - 1.5)$	$\boldsymbol{\sigma_{SF} = 6}$

Figure 4.2: Path Loss model for UMa

4.5.1 RACH success probability $(P(success))$

We define RACH success probability $P(success)$ as the conditional probability that the transmitted preamble by an UE at any given instance, does not encounter collision, given that the preamble is detected at gNB.

For simulations, we simulate in the same area with the user moving using Gauss-Markov mobility model. After the beam failure has been declared, UE will loose connection to the gNB and the beam pairs formation breaks. In order to initiate PRACH and transmit preamble, beam pair formation is required. Unless, the path-loss experienced by UE is below the threshold Ω described in Section. 4.5, UE will not form beam pair with gNB. As soon as the UE is in the good signal region, UE will form a beam-pair with gNB and initiate RACH. For initating RACH, UE selects randomly any one of the 64 available preambles, and transmits it to gNB. If the preamble is detected at the gNB accurately we declare that RACH procedure is successful, with the assumption that MSG- II to IV are successfully decoded.For multiple users, the preamble transmission may occur at same time, at this all the UEs will transmit preambles at same time randomly selected from the same pool of 64 preambles. It may so happen that the same preamble is selected by multiple UEs and transmitted.If detected at gNB, this will cause a preamble collision and RACH failure will be declared.

Chapter 5

Results

In this chapter we present the simulation results produced to show the performance of different preamble sequences in terms of Peak to Average Power Ratio (PAPR) and Cubic Metric (CM) in Section 5.1. Then we show the effect of threshold on the false detection of a preamble for different diversity combining cases in Section 5.2. Further, we discuss the $NLOS$, beam failure performance in Section 5.3. Using these results, we determine the probability of a RACH request being successful in an attempt.

5.1 PAPR and Cubic Metric

. In Fig. 5.1, we see that the ZC sequence perform better than mZC,aZC and $mALL$ sequences. At 99% of sequences we have 6.6dB, 6.8dB,7.1dB and 7.05 dB for ZC, aZC, mZC sequences respectively. This is a very marginal change and can be accommodated if compared with other data signals. In Fig. 5.2, we observe that for CM values between -1dB to 1dB, ZC sequences perform better than mZC,ZC

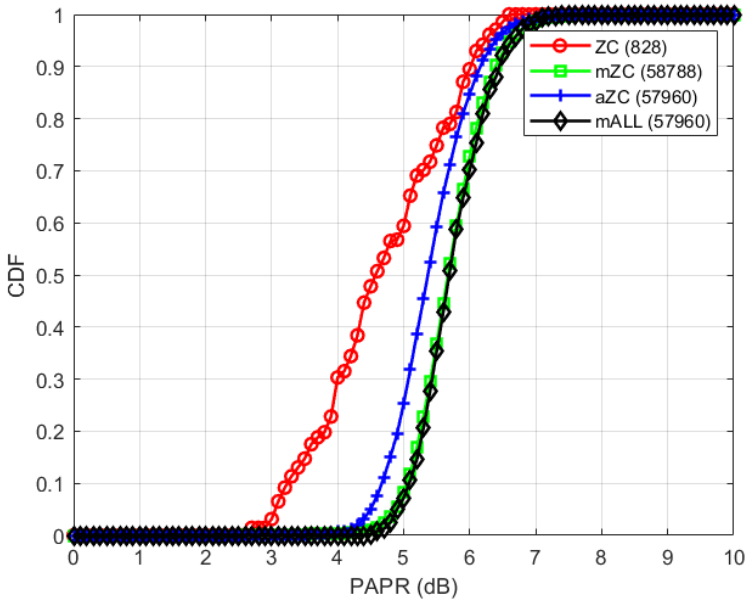

Figure 5.1: CDF of PAPR for ZC, mZC, aZC, $mALL$ sequences

and $mALL$. But considering at 50%, all sequences perform equally at 1.2dB. We see a difference in performance at 99%, where mZC and $mALL$ sequence reaches at 1.8dB,aZC sequence reaches at 1.9dB,mZC sequence reaches at 2.4dB.

From Fig. 5.1,5.2, it is observed that for a negligible performance loss in PAPR, we have increased capacity for preambles. Also, the CM performance of mZC, aZC and $mALL$ is better than ZC by 0.6dB, 0.5dB and 0.6dB respectively.

5.2 $P(detect)$ and η measurement

5.2.1 Threshold Estimation

Based on Section 4.1.2 and 2.3.7, we calculate the threshold to be set considering for each different sequence in consideration and N_{Ant}. For simulations, we consider the

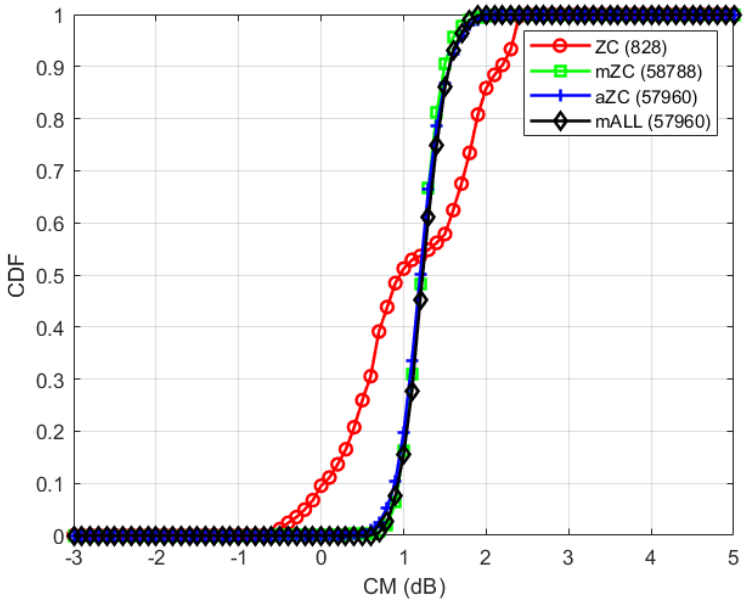

Figure 5.2: CDF of cubic metric (CM) for ZC, mZC, aZC, $mALL$ sequences

signal received as AWGN noise only. Then we correlate the recived noise signal with all root sequences present and by varying threshold, make a decision for detection. In Fig. 5.3, we observe that as the Threshold increases the $P(false)$ decreases. Is is found that to satisfy the condition of $P(false) \leq 0.1\%$, we have Threshold defined in Table 5.1. We observe that there is variation of η for lower N_{Ant} values but as N_{Ant} increase, the η is same for all four sequences.

Sequences	η (N_{Ant}=**2**)	η (N_{Ant}=**4**)	η (N_{Ant}=**8**)
ZC	8.4	5.4	3.8
mZC	8.2	5.3	3.8
aZC	8	5.3	3.8
$mALL$	8.4	5.4	3.8

Table 5.1: Threshold (η) satisfying $P(false)$ condition

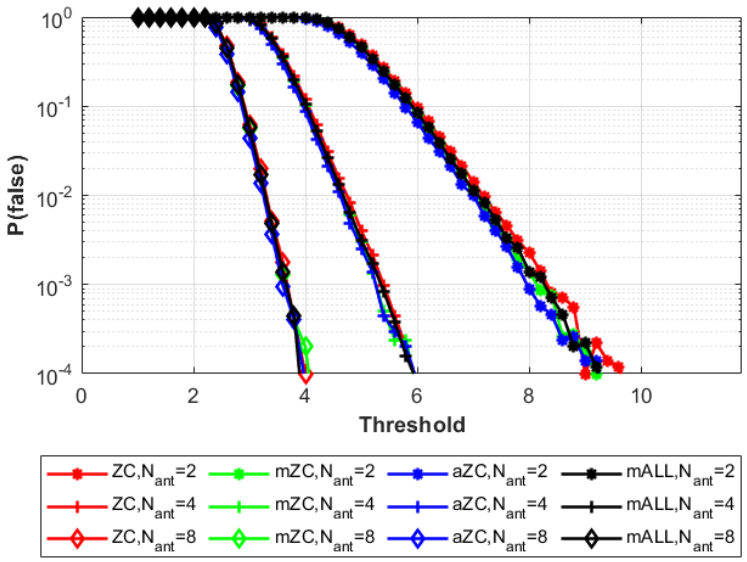

Figure 5.3: Estimating threshold for P(false) $\leq 0.1\%$

5.2.2 $P(detect)$ for single receiver antenna

We use the configuration of single transmit and single receive antenna for this analysis.The parameter $zeroCorrelationZoneConfig$ is set to 11. The $P(detection)$ is calculated using the detection method described in Section 4.1 and values of η taken from Table. 5.1. In Fig. 5.4, we observe that ZC, mZC, aZC and $mALL$ sequence achieve $P(detect)$ of 99% at -7.5 dB, -7.15 dB, -7.2 dB and -7.25 dB respectively. ZC sequence detection performance is better than other sequences. Worst detection performance is given by mZC sequences. Proposed sequence $mALL$ detection is better than mZC and aZC by 0.1 dB and 0.5 dB respectively.

5.2.3 $P(detect)$ with equal gain combining

In Fig. 5.5, the detection performance has been observed in AWGN channel for a single user case, varying N_{Ant} as 2,4 and 8. We assume no Doppler shift.There

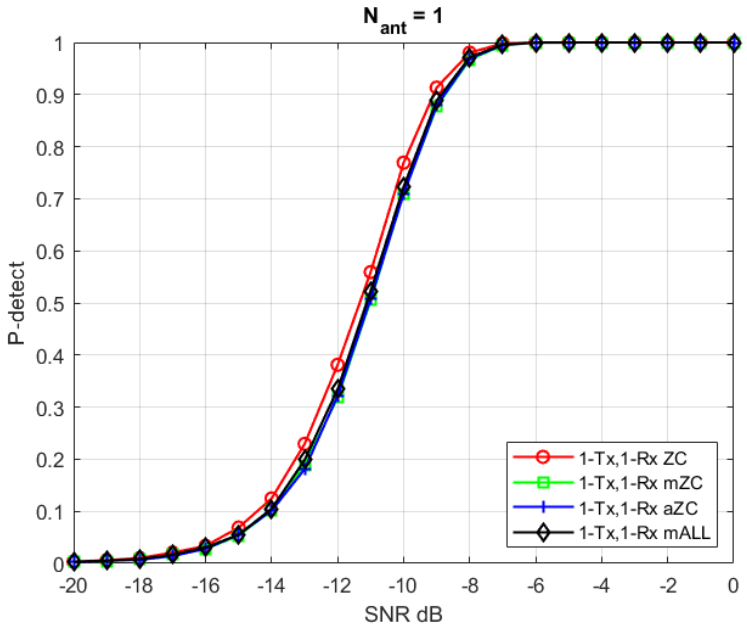

Figure 5.4: $P(detection)$ for ZC, mZC, aZC, $mALL$ for 1-TX,1-RX configuration

are no repeated transmissions of the preamble sequences as given in formats for preamble transmission. Threshold η is taken from Table 5.1. We observe that there is no deviation in performance of detection with respect to varying SNR for all the four sequences considered namely ZC, mZC, aZC and $mALL$. But varying N_{Ant} has effect on the performance.All the four sequences perform similarly for same threshold calculation for different number of antennas. But,as the number of antennas increase we find a performance improvement in the detection. This behaviour can be attributed to the diversity combining of antennas to give us a more accurate detection.

In Fig. 5.5, for lower SNR in the range of -20 to -16 dB, $N_{ant} = 8$ and $N_{ant} = 4$ systems perform 3dB and 1dB better than $N_{ant} = 2$ system, respectively. When achieving the $P(detect)$ greater than 99%,$N_{ant} = 8$ and $N_{ant} = 4$ systems perform better than $N_{ant} = 2$ system, by 4.6dB and 2.1dB respectively. This is an significant improvement we see using the diversity combing. Note, that the performance for

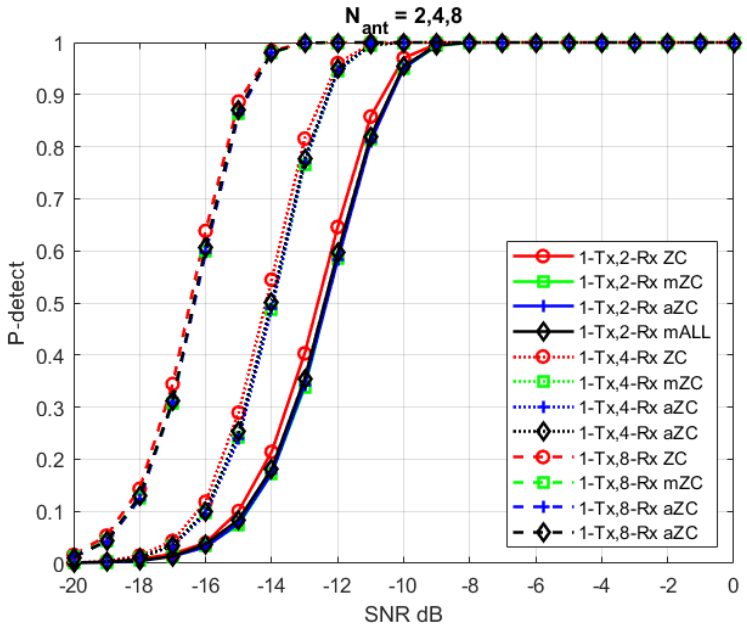

Figure 5.5: Comparison of $P(detection)$ for ZC, mZC, aZC, $mALL$ sequences varying SNR and N_{Ant}

legacy ZC sequence is always marginally better than that of other three sequences and the proposed $mALL$ sequence also perform marginally better than mZC and aZC sequence. It is also observed that as N_{Ant} increases, the performance gap of mZC,aZC,$mALL$ with ZC sequence reduces.

5.3 $P(NLOS), P(failure)$ and $P(success)$

5.3.1 $P(NLOS)$

Fig.5.6, shows the probability of a UE being in N-LOS at any given instance. It is observed that varying the obstacle density, we see a change in P-NLOS. Specifically, increasing the obstacle density increase the P-NLOS. The curve pf P-NLOS, on

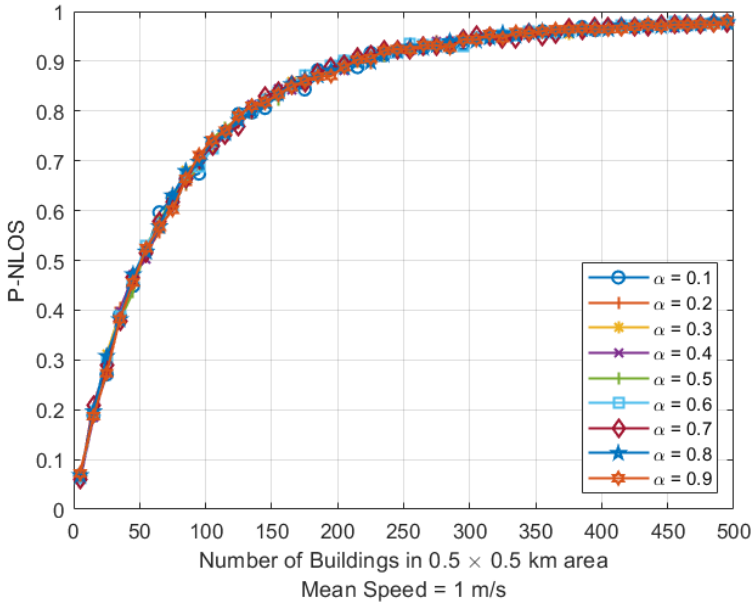

Figure 5.6: Effect of α on Probability of NLOS condition

initial observations, may mimic the curve of $1 - \exp(-\beta x)$. The probability of a UE being in NLOS state, saturates close to 1, for a building density of 500 buildings in the given area. This is to be expected, as the number of building are very high in the given area, the UE will tend to remain in N-LOS state for all the time. This in turn, validates our system model. The effect of tuning parameter α, defined in 4.3 is also observed. It is observed that varying the tuning parameter α in (4.3.1) from 0.1 to 0.9 does not affect the NLOS probability in any way. Thus the effect of α can be neglected.

From Fig.5.7,it is observed that the mean-speed also does not have any effect on the trend of increasing $P(NLOS)$ with obstacle density. Increasing the speed does not, in any case, divert from the expected NLOS probability. This factor can be attributed to the fact that for each iteration, UE is initialised at uniformly distributed position and direction, which result in accounting for all the locations in a given area, irrespective of UE speed.

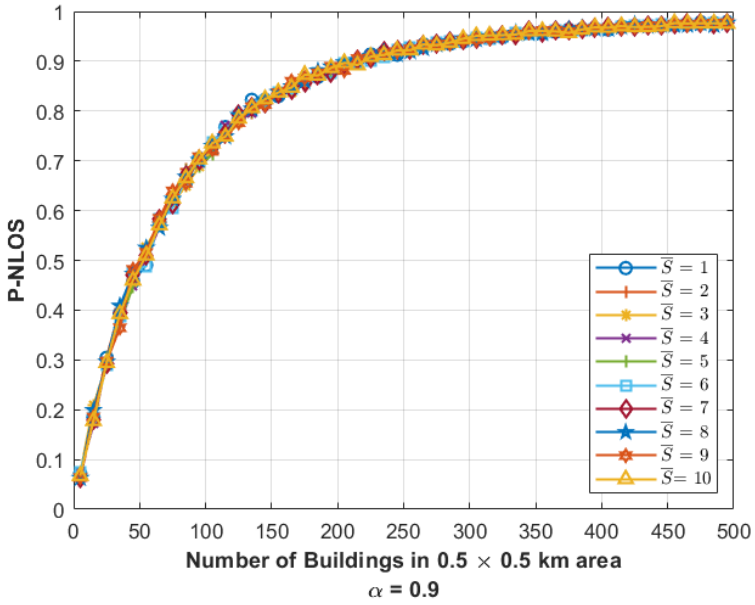

Figure 5.7: Effect of mean speed on Probability of NLOS condition

5.3.2 $P(failure)$

The values used for calculation for path loss from (4.5.1) (4.5.2) and Fig4.2 are given in Table.4.2

Fig.5.8 shows the probability of beam failure across increasing obstacle density and increasing speed.We observe that the beam failure probability saturation depends only on obstacle density. As we increase speed from 1 to 7 m/s, the probability beam failure is higher for higher speed in the range of 5-350 obstacle density. At higher obstacle density above 350, we see the $P(failure)$ starts to saturate at about 3.5%. Looking at same data from different perspective, Fig.5.9, we deduce that, as obstacle density increases, the effect of speed on probability of beam-failure reduces.

The trend for $P(failure)$ in 5.8, is similar to the trend observed for $P(NLOS)$ for lower speeds. But for higher speeds, $P(failure)$ achieves a peak before saturating for medium obstacle density. This behaviour can be attribute to the fact that, for moderate obstacle density, as the speed increases, the UE tends to switch from LOS

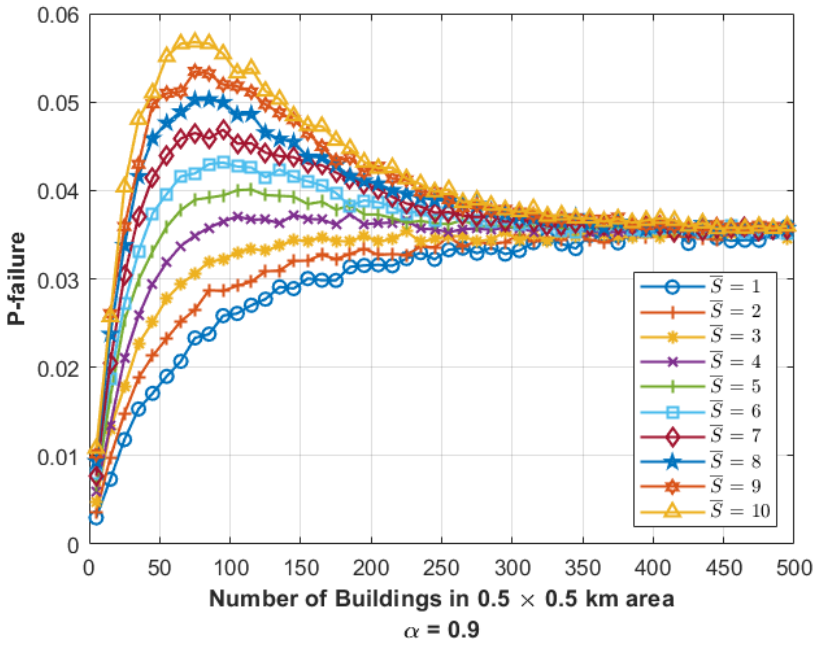

Figure 5.8: Effect of mean speed on Probability of Beam Failure

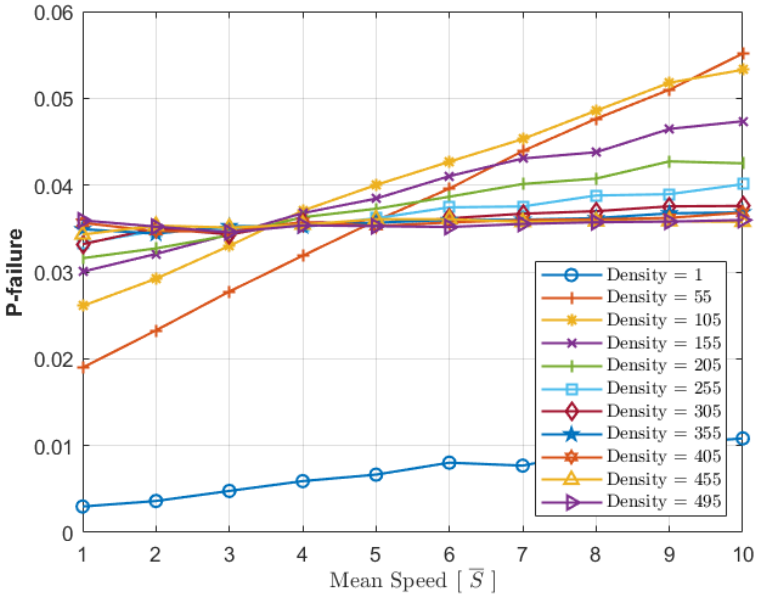

Figure 5.9: Effect of Obstacle density on Probability of Beam Failure

to NLOS state more frequently and vice-versa. This increase the chance of UE going beyond the path loss threshold Ω for a certain time, thus counting towards higher $P(failure)$. As for higher obstacle density, as the $P(NLOS)$ is very high, irrespective of the speed, the UE tends to remain beyond path loss threshold Ω for a long periods of time, where we count the beam-failure instance less frequently.

Chapter 6

Conclusion and Future Scope

6.1 Conclusion

We compared ZC sequence detection performance with proposed sequences in literature namely, mZC and aZC. We find that the performance of detection is very similar for all the three sequences using same detection technique. We propose a new candidate sequence $mALL$ for preamble generation for RACH. Proposed sequence shows similar detection performance and cubic metric performance compared with other sequences such as ZC, mZC *and* aZC, but with higher $PrCapacity$ than any other sequences. It is observed that the detection performance of ZC sequence is marginally better than $mZC, aZC, mALL$ sequence but with a trade-off of lower $PrCapacity$. The Cubic metric performance of ZC is worse than other sequences. Thus with a marginal trade-off for detection performance we achieve higher $PrCapacity$ for the candidate sequences considered.

In simulations for Part-II, we observe that $P(NLOS)$ increases with increase in obstacle density and it starts to saturate to 100% at high obstacle densities. This

is to be expected since a very high obstacle density will result in a UE to be always in NLOS state. It is observed that the value of tuning parameter α, used in Gauss-Markov mobility model does not have any effect on the $P(NLOS)$ trend. Similarly, it is observed that the increase in mean-speed $\overline{S}$, also does not have any effect on the $P(NLOS)$ trend. For $P(failure)$, it is observed, that as the speed increases, the $P(failure)$ increases with speed for moderate obstacle densities. BUt for higher obstacle densities, the effect of speed is negated and $P(failure)$ saturates at 0.35.

6.2 Future Scope

The effect of multipath and Doppler Shift on the preamble detection for the proposed sequence is remaining to be seen. Analysis of reuse factor also remains to be explored. The impact of increased $PrCapacity$ on SINR and collisions can be explored in detail. In our work, we consider that UEs are blocked due to buildings and other obstacles. In addition, self blockage and the blockage due to other UEs can be included in the model. As of now, we consider the UEs to be mobile, and the blockages are static, which can be further extended to include a mobility model for obstacles too to consider the blockage created by vehicles.

Bibliography

[1] J. Campos, "Understanding the 5g nr physical layer," *Keysight Technologies release*, 2017.

[2] "3GPP,Study on channel model for frequencies from 0.5 to 100 GHZ (Release 16)," Technical Report (TR) 38.901, November 2020, version 16.1.0.

[3] R. Frank, S. Zadoff, and R. Heimiller, "Phase shift pulse codes with good periodic correlation properties (corresp.)," *IRE Transactions on Information Theory*, vol. 8, no. 6, pp. 381–382, 1962.

[4] D. Chu, "Polyphase codes with good periodic correlation properties (corresp.)," *IEEE Transactions on information theory*, vol. 18, no. 4, pp. 531–532, 1972.

[5] G. Schreiber and M. Tavares, "5g new radio physical random access preamble design," in *2018 IEEE 5G World Forum (5GWF)*. IEEE, 2018, pp. 215–220.

[6] A. E. Mostafa, V. W. Wong, S. Liao, R. Schober, M. Ding, and F. Wang, "Aggregate preamble sequence design for massive machine-type communications in 5g networks," in *2018 IEEE Global Communications Conference (GLOBECOM)*. IEEE, 2018, pp. 1–6.

[7] J. M. P. Arana, K. M. Saquib, and Y. S. Cho, "Random access preamble design for 5g millimeter-wave cellular systems with multiple beams," in *2017 Ninth*

International Conference on Ubiquitous and Future Networks (ICUFN). IEEE, 2017, pp. 378–380.

[8] R.-A. Pitaval, B. M. Popovic, F. Berggren, and P. Wang, "Overcoming 5g prach capacity shortfall by combining zadoff-chu and m-sequences," in *2018 IEEE International Conference on Communications (ICC)*. IEEE, 2018, pp. 1–6.

[9] R.-A. Pitaval, B. M. Popović, P. Wang, and F. Berggren, "Overcoming 5g prach capacity shortfall: Supersets of zadoff–chu sequences with low-correlation zone," *IEEE Transactions on Communications*, vol. 68, no. 9, pp. 5673–5688, 2020.

[10] F. Bai, N. Sadagopan, and A. Helmy, "The important framework for analyzing the impact of mobility on performance of routing protocols for adhoc networks," *Ad hoc networks*, vol. 1, no. 4, pp. 383–403, 2003.

[11] M. J. Alenazi, S. O. Abbas, S. Almowuena, and M. Alsabaan, "Rssgm: Recurrent self-similar gauss–markov mobility model," *Electronics*, vol. 9, no. 12, p. 2089, 2020.

[12] S. Sun, T. S. Rappaport, S. Rangan, T. A. Thomas, A. Ghosh, I. Z. Kovacs, I. Rodriguez, O. Koymen, A. Partyka, and J. Jarvelainen, "Propagation path loss models for 5g urban micro-and macro-cellular scenarios," in *2016 IEEE 83rd Vehicular Technology Conference (VTC Spring)*. IEEE, 2016, pp. 1–6.

[13] H. Tataria, K. Haneda, A. F. Molisch, M. Shafi, and F. Tufvesson, "Standardization of propagation models for terrestrial cellular systems: A historical perspective," *International Journal of Wireless Information Networks*, vol. 28, no. 1, pp. 20–44, 2021.

[14] M. Giordani, M. Polese, A. Roy, D. Castor, and M. Zorzi, "A tutorial on beam management for 3gpp nr at mmwave frequencies," *IEEE Communications Surveys & Tutorials*, vol. 21, no. 1, pp. 173–196, 2018.

[15] Y.-N. R. Li, B. Gao, X. Zhang, and K. Huang, "Beam management in millimeter-wave communications for 5g and beyond," *IEEE Access*, vol. 8, pp. 13 282–13 293, 2020.

[16] "3GPP,Technical Specification Group Radio Access Network (Release 16)," Technical Specification (TS) 38.211, September 2020, version 16.3.0.

[17] A. Behravan and T. Eriksson, "Some statistical properties of multicarrier signals and related measures," in *2006 IEEE 63rd Vehicular Technology Conference*, vol. 4. IEEE, 2006, pp. 1854–1858.

[18] X. Zhu, H. Hu, Z. Meng, and J. Xia, "On minimizing the cubic metric of ofdm signals using convex optimization," *IEEE Transactions on Broadcasting*, vol. 60, no. 3, pp. 511–523, 2014.

[19] Y. Huang, R. Yang, and B. Su, "Reducing cubic metric of circularly pulse-shaped ofdm signals through constellation shaping optimization with performance constraints," in *2018 IEEE 88th Vehicular Technology Conference (VTC-Fall)*. IEEE, 2018, pp. 1–6.

[20] "3GPP,Base Sation (BS) radio transmission and reception (Release 16)," Technical Specification (TS) 38.104, November 2020, version 16.5.0.

[21] B. M. Popovic, "Quasi-orthogonal supersets," in *2011 IEEE Information Theory Workshop*. IEEE, 2011, pp. 155–159.

[22] W. Alltop, "Complex sequences with low periodic correlations (corresp.)," *IEEE Transactions on Information Theory*, vol. 26, no. 3, pp. 350–354, 1980.

[23] R. W. Heath, T. Strohmer, and A. J. Paulraj, "On quasi-orthogonal signatures for cdma systems," *IEEE Transactions on Information Theory*, vol. 52, no. 3, pp. 1217–1226, 2006.